PRAMANA
— journal of
physics

Vol. 73, No. 3
September 2009
pp. 543–551

Resonance eigenfunctions in chaotic scattering systems

MARTIN SIEBER
School of Mathematics, University of Bristol, Bristol BS8 1TW, United Kingdom
E-mail: M.Sieber@bristol.ac.uk

Abstract. We study the semiclassical structure of resonance eigenstates of open chaotic systems. We obtain semiclassical estimates for the weight of these states on different regions in phase space. These results imply that the long-lived right (left) eigenstates of the non-unitary propagator are concentrated in the semiclassical limit $\hbar \to 0$ on the backward (forward) trapped set of the classical dynamics. On this support the eigenstates display a self-similar behaviour which depends on the limiting decay rate.

Keywords. Resonances; semiclassics; quantum chaos.

PACS Nos 05.45.Mt, 03.65.Sq, 05.45.Df

1. Introduction

The Schrödinger equation has different types of solutions in open and closed quantum systems. In closed systems the quantum Hamiltonian has a discrete spectrum with normalizable eigenfunctions, whereas in open systems one has scattering solutions with a corresponding continuous spectrum, and possibly additional bound states. In scattering systems one can, however, alternatively consider quantum resonances instead of scattering solutions. These resonances can play a similar role in open systems as the eigenstates in closed systems, for example for the time-development of general quantum states or in semiclassical trace formulas [1].

Resonances are poles of the Green function $G(x, x', E) = \langle x|(E - \hat{H})^{-1}|x'\rangle$ in the lower half-plane Im $E < 0$ to which the Green function can be meromorphically continued. The corresponding resonance eigenfunctions can be obtained from the residues of the poles. Alternatively, one can obtain resonances and corresponding eigenfunctions as complex energy solutions of the Schrödinger equation with outgoing boundary conditions. The resonances coincide also with the poles of the scattering matrix.

There are a number of immediate questions about properties of resonances: What are the number and distribution of resonances in regions of the complex energy plane? How are resonance eigenstates typically distributed in phase space? What are the classical objects that are relevant for these questions in the semiclassical limit $\hbar \to 0$?

In closed systems the answers to similar questions are well established. The Thomas Fermi or Weyl formula gives the asymptotic number of energy levels below energy E

$$\#\{E_n \leq E\} \sim \frac{1}{(2\pi\hbar)^f} \int \mathrm{d}^f q \, \mathrm{d}^f p \, \Theta(E - H(\mathbf{q}, \mathbf{p})) \quad \text{as } \hbar \to 0, \tag{1}$$

where f is the number of degrees of freedem and $\Theta(z)$ is the Heaviside theta function. It implies that there is asymptotically one eigenstate per Planck cell $(2\pi\hbar)^f$ in phase space.

In the case of chaotic systems there are rigorous semiclassical results for eigenfunctions. The quantum ergodicity theorem states that the Wigner function of almost all eigenstates concentrates in the semiclassical limit on the energy shell in phase space [2]. This is the region that is explored by a typical trajectory of the classical system [3].

Much less is known about open chaotic systems. It is assumed that the number of resonances near some real energy E follows a fractal Weyl law [1,4], but a proof exists only for one model system [5]. In this article we will concentrate on properties of resonance eigenstates [6–9]. We will investigate them by modelling the interaction region of a chaotic scattering system by simple quantum maps. The article is mainly based on [7], but contains some extensions and new numerical results. In §2 we first discuss classical properties of open chaotic maps, whereas the quantum versions are discussed in §3.

2. The trapped sets

As discussed in the introduction, the energy surface is the classical set that determines the density of energy levels as well as the distribution of eigenstates of closed chaotic systems in the semiclassical limit. In contrast, one finds that in open chaotic systems only parts of the energy surface are important. These are the so-called trapped sets. One distinguishes between the forward trapped set K_- which consists of points in phase space which never leave the system as $t \to \infty$, and the backward trapped set K_+ which are points that remain trapped when propagated backwards in time as $t \to -\infty$. The intersection of both sets is the trapped set. In chaotic systems the trapped set is typically a repeller with a fractal dimension.

These sets have, in general, a very complicated structure. In order to make progress one studies simple model systems such as chaotic maps which act on a compact phase space in the form of the unit torus $(q, p) \in T = [0, 1) \times [0, 1)$. A particularly convenient model is the baker map because its backward and forward trapped sets have a very simple structure. The closed triadic baker map is defined by

$$\mathcal{U}(q,p) = \begin{cases} \left(3q, \frac{p}{3}\right) & \text{if } \ 0 \leq q < \frac{1}{3}, \\ \left(3q-1, \frac{p+1}{3}\right) & \text{if } \ \frac{1}{3} \leq q < \frac{2}{3}, \\ \left(3q-2, \frac{p+2}{3}\right) & \text{if } \ \frac{2}{3} \leq q < 1, \end{cases} \tag{2}$$

and figure 1 illustrates one iteration of the map.

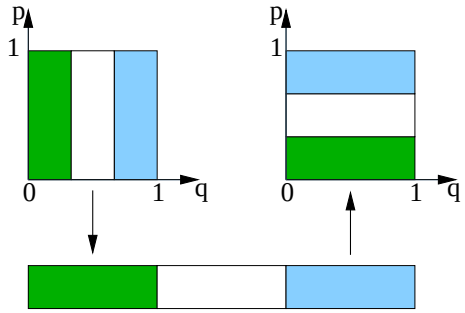

Figure 1. One time step of the triadic baker map consists of stretching in q-direction and compressing in p-direction, followed by stacking the pieces on top of each other.

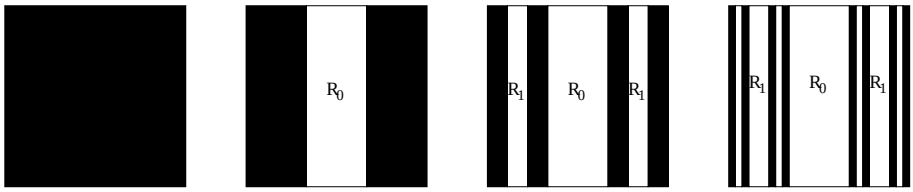

Figure 2. Construction of the forward trapped set of the open baker map.

The map is opened up by choosing an area in phase space as an opening $\mathcal{O}$. Points in the opening are removed from the system in the next time step. The opening is usually chosen as a strip parallel to the p-axis in phase space. The open map might be considered as a model for the bouncing map of a cavity with an opening, for example in the form of an attached perfect lead. We choose the middle third of the triadic baker map as opening, i.e. the white region in figure 1.

In order to find the trapped sets one considers the backward and forward images of the opening $\mathcal{O}$. The nth image of the opening under the classical map is denoted by $\mathcal{O}_n = \mathcal{U}^n(\mathcal{O})$, $n \in \mathbf{Z}$, where $\mathcal{O}_0 = \mathcal{O}$ in this notation.

The forward trapped set K_- is obtained by removing the opening and all its pre-images from phase space. This is done iteratively in figure 2. At each time step the vertical middle third of each remaining black region is removed. The limit of this proceedure is $K_- = \text{Can} \times [0, 1)$ where Can is the middle third Cantor set.

The white regions in figure 2 are set of points that are mapped into the hole after a finite number of time steps. Let $\mathcal{R}_m$ be the set of points which fall into the hole after m time steps, but not earlier

$$\mathcal{R}_m = \{x \in \mathcal{O}_{-m},\, x \notin \mathcal{O}_{-l},\, 0 \leq l < m\}, \tag{3}$$

with the convention that $\mathcal{R}_0 = \mathcal{O}$. The set $\mathcal{R}_m$ consists of 2^m separate parts, and $\mathcal{R}_0$ and $\mathcal{R}_1$ are labelled in the figure. One can show that the sets are related by

$$\mathcal{U}^{-1}(\mathcal{R}_m) \backslash \mathcal{O} = \mathcal{R}_{m+1}, \quad m = 0, 1, 2, \ldots. \tag{4}$$

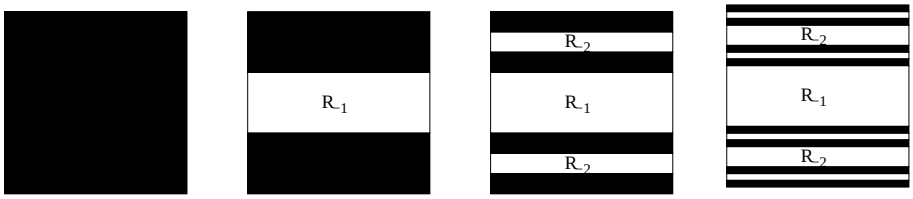

Figure 3. Construction of the backward trapped set of the open baker map.

It is clear that one can partition the phase space into sets of points that fall into the hole after m time steps, where $m = 0, 1, 2, \ldots$, or never. This results in the forward partition of the phase space

$$T = \left(\bigcup_{m=0}^{\infty} \mathcal{R}_m \right) \cup K_- \,. \tag{5}$$

The backward trapped set is obtained in a similar way by removing all forward images of the hole from phase space. This is done iteratively in figure 3. In comparison to the forward trapped set one sees that position and momentum coordinates are simply interchanged. The procedure results in the backward trapped set $K_+ = [0, 1) \times \mathrm{Can}$.

Similarly as before, one can also define sets of points $\mathcal{R}_{-m}$ by

$$\mathcal{R}_{-m} = \{x \in \mathcal{O}_m,\, x \notin \mathcal{O}_l,\, 1 \leq l < m\} \,. \tag{6}$$

They consist of 2^{m-1} different parts, and the first two sets $\mathcal{R}_{-1}$ and $\mathcal{R}_{-2}$ are labelled in figure 3. Consecutive sets are related by

$$\mathcal{U}(\mathcal{R}_{-m} \backslash \mathcal{O}) = \mathcal{R}_{-m-1}, \quad m = 1, 2, \ldots, \tag{7}$$

and together with K_+ they yield the backward partition of phase space

$$T = \left(\bigcup_{m=1}^{\infty} \mathcal{R}_{-m} \right) \cup K_+ \,. \tag{8}$$

The sets $\mathcal{R}_m$, $m \in \mathbf{Z}$, will be important in the next section, because one can obtain semiclassical estimates for the weight of resonance eigenstates on these regions. Finally, we remark that

$$\mathcal{U}^{-1}(\mathcal{R}_1) \backslash \mathcal{O} = \emptyset \,. \tag{9}$$

3. The resonance states

The quantization of the closed baker map specifies a unitary propagator that acts on an N-dimensional Hilbert space. The dimension N defines an effective Planck's constant $\hbar = (2\pi N)^{-1}$, and the semiclassical limit corresponds to $N \to \infty$. For the

triadic baker map we require that N is a multiple of 3. The propagator is given by [10,11]

$$U = F_N^\dagger \begin{pmatrix} F_{N/3} & & \\ & F_{N/3} & \\ & & F_{N/3} \end{pmatrix}, \tag{10}$$

where F_N is a discrete Fourier transform

$$(F_N)_{nm} = \frac{1}{\sqrt{N}} \mathrm{e}^{-\frac{2\pi \mathrm{i}}{N}(n+1/2)(m+1/2)}, \quad n, m \in \{0, \ldots, N-1\}. \tag{11}$$

This choice of quantization corresponds to antiperiodic boundary conditions which preserve the time-reversal symmetry and parity symmetry of the system. Both the position and momentum eigenstates have half-integer eigenvalues $n - 1/2$ where $n = 1, \ldots, N$.

The open quantum map is obtained by multiplying the propagator from the right with the projector onto the complement of the opening [5,12]

$$\widetilde{U} = F_N^\dagger \, \mathrm{diag}(F_{N/3}, F_{N/3}, F_{N/3}) \Pi = F_N^\dagger \, \mathrm{diag}(F_{N/3}, 0, F_{N/3}) \,, \tag{12}$$

where $\Pi = 1 - \Pi_0$, and Π_0 is the projector onto the opening. As a consequence, position states that are located in the hole are destroyed by the application of the propagator.

The propagator $\widetilde{U}$ of the open map is a subunitary matrix with eigenvalues inside the unit circle, $|\lambda_n| \leq 1$. The left and right eigenvectors are in general different:

$$\widetilde{U} \, |\psi_n^{\mathrm{R}}\rangle = \lambda_n |\psi_n^{\mathrm{R}}\rangle \,, \quad \langle \psi_n^{\mathrm{L}}| \, \widetilde{U} = \lambda_n \langle \psi_n^{\mathrm{L}}| \,, \quad n = 1, \ldots, N \,. \tag{13}$$

We assume that $\langle \psi_n^{\mathrm{R}} | \psi_n^{\mathrm{R}} \rangle = \langle \psi_n^{\mathrm{L}} | \psi_n^{\mathrm{L}} \rangle = 1$. The open triadic baker map has the special property that the position representation of the left eigenvectors is equal to the momentum representation of the right eigenvectors. For this reason, we will concentrate in the remaining part of the article on the right eigenstates.

Before we look at numerical results, let us discuss what properties we expect for eigenvalues and eigenvectors of $\widetilde{U}$. We know that one third of the eigenvalues of $\widetilde{U}$ are identical to zero, because they correspond to position states which are located in the opening. But there are many other states whose eigenvalues are very close to zero. These are short-lived states which leave the system in times shorter than the Ehrenfest time $t_{\mathrm{E}} = \log(N/3)/\log 3$, the time it takes for a minimal wave packet to spread to the size of the opening. An estimate of the number of these short-lived states was used for an explanation of the fractal Weyl law in [13]. For longer-lived states we have predictions on how they are distributed in phase space. These are based on semiclassical estimates for the weight of these states on the regions $\mathcal{R}_m$.

Let us denote by Π_m the projection operators onto the regions $\mathcal{R}_m$ for $m \in \mathbf{Z}$. These are examples of the general class of projectors in [14,15]. We obtain the projector onto the opening $\mathcal{R}_0$ from the definition of $\widetilde{U} = U\Pi$

$$\Pi_0 = 1 - \widetilde{U}^\dagger \widetilde{U} \,. \tag{14}$$

For times shorter than the Ehrenfest time we expect that the quantum evolution can be modelled by the classical evolution. The quantum version of the relation (4) is given by $\Pi_{m+1} \approx \widetilde{U}^\dagger \Pi_m \widetilde{U}$. Together with (14) and (13) this yields the following result for the weight on the regions $\mathcal{R}_m$ for $m \geq 0$ [7]:

$$\langle \psi_n^{\mathrm{R}} | \Pi_m | \psi_n^{\mathrm{R}} \rangle \approx |\lambda_n|^{2m} (1 - |\lambda_n|^2). \tag{15}$$

We expect this to hold if m is smaller than the Ehrenfest time. Relation (15) was numerically investigated in [7]. In the present article we will concentrate on the projection operators Π_m for negative m.

The starting point is the projector onto $\mathcal{R}_1$

$$\Pi_{-1} = 1 - \widetilde{U}\widetilde{U}^\dagger. \tag{16}$$

This representation is exact for the open triadic baker map. The quantum version of the classical relation (7) is $\Pi_{-m-1} \approx \widetilde{U} \Pi_{-m} \widetilde{U}^\dagger$. This can be used to obtain the weight of left eigenstates on the regions $\mathcal{R}_{-m}$. For the right eigenstates it is more useful to consider the quantum version of (9) which is $\widetilde{U}^\dagger \Pi_{-1} \widetilde{U} = 0$, or its generalization $(\widetilde{U}^\dagger)^m \Pi_{-m} \widetilde{U}^m \approx 0$. We take the expectation value on both sides of this relation and obtain

$$|\lambda_n|^{2m} \langle \psi_n^{\mathrm{R}} | \Pi_{-m} | \psi_n^{\mathrm{R}} \rangle \approx 0, \quad m > 0. \tag{17}$$

This states that the weight of the right eigenstates on the regions $\mathcal{R}_{-m}$ is approximately zero unless the eigenstates are short-lived $|\lambda_n| \approx 0$. Again we expect this to hold if m is smaller than the Ehrenfest time. The estimate (17) implies that the long-lived right eigenstates are concentrated on the backward trapped set within the resolution set by the finite value of $\hbar$ [7,8]. It was shown in [8] that the localization properties of resonance states (see (15) and (17)) can be associated with conditionally invariant measures. These are measures that are only invariant up to a constant factor, the decay rate [16].

We will now investigate numerically some of these semiclassical results for the open triadic baker map. We choose a Hilbert space dimension $N = 3027$. We avoid a power of 3 in order to rule out special effects as in [17]. As the first result we plot in figure 4 the number $N(\rho)$ of eigenstates with eigenvalue $|\lambda_n| \leq \rho$. One sees that a majority of eigenstates have eigenvalues very close to zero. These are the short-lived states.

We are interested in the properties of the long-lived states. For a first illustration we calculated the Husimi functions of the 100 longest-lived states. A formula for the Husimi function can be found in [18]. The average of these 100 functions is presented in figure 5. One can see that the average is very nicely concentrated on the backward trapped set within the resolution set by the finite value of $\hbar$.

We investigate now the weight of the eigenstates on the regions $\mathcal{R}_{-m}$ in more detail. According to eq. (17) this weight should be approximately zero for long-lived states as long as m is smaller than the Ehrenfest time. Figure 6 shows the result of a numerical evaluation for the cases $m = 1$–4. The horizontal lines present the weight that one would expect if the states were evenly distributed over the phase space. The results are in agreement with the expectation. Only the very short-lived states with $|\lambda_n| \approx 0$ have a considerable weight on the regions $\mathcal{R}_{-m}$. All the

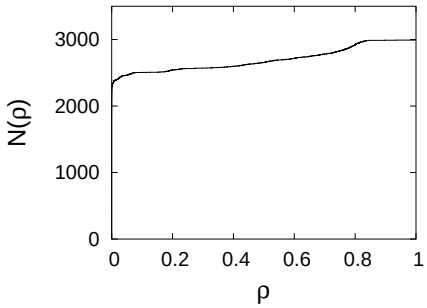

Figure 4. Number $N(\rho)$ of eigenstates with eigenvalue $|\lambda_n| \leq \rho$, $N = 3027$.

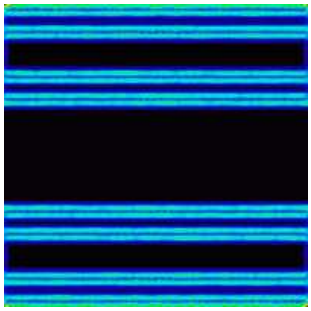

Figure 5. Average of Husimi functions of 100 longest-lived states, $N = 3027$. Intensity increases from dark to light.

other resonance states have a very small weight there. One can further see that the long-lived states which agree best with the semiclassical expectation (zero weight on $\mathcal{R}_{-m}$) are those with smaller eigenvalue modulus. This was also observed in numerical results for weights on the regions $\mathcal{R}_m$ with positive m in [7].

Finally, we consider the position representation of the eigenstates. In figure 7 we present numerical results for an average of 100 eigenstates with eigenvalue modulus near 0.7. The probability density exhibits a remarkable degree of self-similarity. Although the semiclassical results for the weights on the regions $\mathcal{R}_m$ in eq. (15) are consistent with a self-similar behaviour they do not imply it. So far, self-similar behaviour has been proved only for a special version of the quantum baker map, the Walsh quantized baker map [9]. This is a model which can be solved explicitly [5], i.e. all eigenvalues and eigenfunctions can be obtained in closed form. Let us mention here that self-similarity has also been observed in a closed chaotic system in which eigenfunctions can be obtained analytically [19].

In summary, we have obtained semiclassical formulas for the weight of resonance eigenfunctions on the regions $\mathcal{R}_m$, $m \in \mathbf{Z}$, in phase space. These regions are related to images and pre-images of the opening. Although we considered the particular example of the open triadic baker map, these formulas are valid more generally. They show that resonance eigenstates of open chaotic systems concentrate on fractal trapped sets [7,8]. On these fractal sets the distribution of the resonance

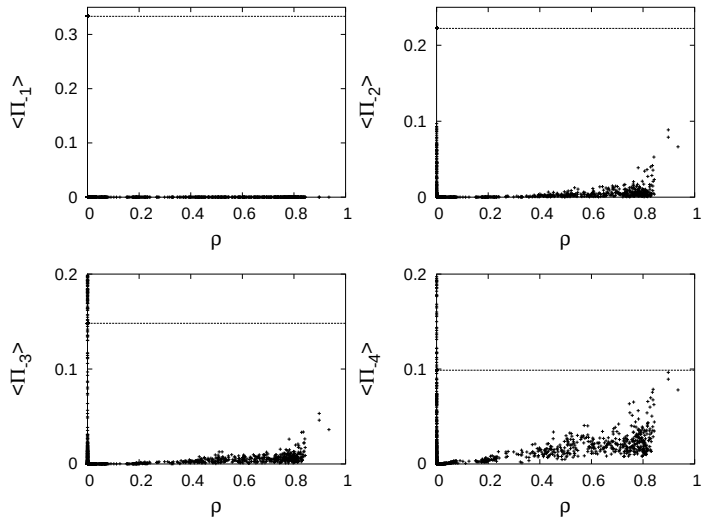

Figure 6. Weight $\langle\psi_n^{\mathrm{R}}|\Pi_{-m}|\psi_n^{\mathrm{R}}\rangle$ of eigenfunctions on the regions $\mathcal{R}_{-m}$, $m = 1, 2, 3, 4$, where ρ is the modulus of eigenvalues. The horizontal lines denote the relative size of the regions $\mathcal{R}_{-m}$ in phase space.

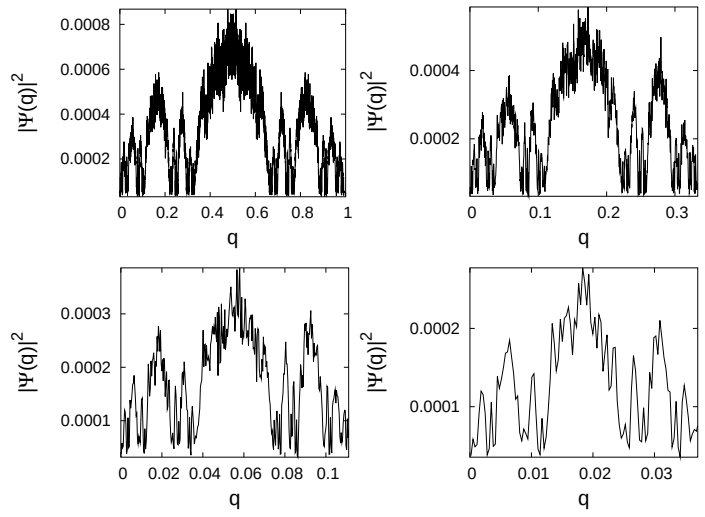

Figure 7. Average of $|\psi_n^{\mathrm{R}}(q)|^2$ for 100 eigenstates with eigenvalue modulus near 0.7. In every subsequent figure, the q-range is decreased by a factor of 1/3, thus demonstrating the self-similarity of the probability distribution.

states depends on the modulus of the eigenvalues, and we found numerically that they display self-similar behaviour. A theoretical derivation of this self-similarity has been obtained so far only for a different model, the Walsh quantized baker map [9].

Acknowledgements

This work was supported by the EPSRC grant EP/C515137/1. The author would like to thank Arul Lakshminarayan for helpful suggestions.

References

[1] M Zworski, *Not. Am. Math. Soc.* **46**, 319 (1999)
[2] A I Shnirelman, *Usp. Mat. Nauk* **29**, 181 (1974)
[3] M V Berry, *J. Phys.* **A10**, 2083 (1977)
[4] J Sjöstand, *Duke Math. J.* **60**, 1 (1990)
[5] S Nonnenmacher and M Zworski, *J. Phys.* **A38**, 10683 (2005)
[6] G Casati, G Maspero and D L Shepelyanski, *Physica* **D131**, 311 (1999)
[7] J P Keating, M Novaes, S D Prado and M Sieber, *Phys. Rev. Lett.* **97**, 150406 (2006)
[8] S Nonnenmacher and M Rubin, *Nonlinearity* **20**, 1387 (2007)
[9] J P Keating, S Nonnenmacher, M Novaes and M Sieber, *Nonlinearity* **21**, 2591 (2008)
[10] N L Balazs and A Voros, *Ann. Phys.* **190**, 1 (1989)
[11] M Saraceno, *Ann. Phys.* **199**, 37 (1990)
[12] M Saraceno and R O Vallejos, *Chaos* **6**, 193 (1996)
[13] H Schomerus and J Tworzydlo, *Phys. Rev. Lett.* **93**, 154102 (2004)
[14] M Saraceno and A Voros, *Physica* **D79**, 206 (1994)
[15] R O Vallejos and M Saraceno, *J. Phys.* **A32**, 7273 (1999)
[16] M F Demers and L-S Young, *Nonlinearity* **19**, 377 (2006)
[17] N Meenakshisundaram and A Lakshminarayan, *Phys. Rev.* **E71**, 065303 (2005)
[18] L Ermann and M Saraceno, *Phys. Rev.* **E78**, 036221 (2008)
[19] S R Jain, B Grémaud and A Khare, *Phys. Rev.* **E66**, 016216 (2002)